Applied Surface Science 255 (2008) 3230–3234

Contents lists available at ScienceDirect

Applied Surface Science

journal homepage: www.elsevier.com/locate/apsusc

Effect of TiO_2 buffer layer on the structural and optical properties of ZnO thin films deposited by E-beam evaporation and sol–gel method

Linhua Xu [a,*], Linxing Shi [b], Xiangyin Li [a]

[a] Department of Applied Physics, Nanjing University of Science and Technology, Xiaolingwei 200, Nanjing 210094, PR China
[b] Department of Mathematics and Physics, Huaihai Institute of Technology, Lianyungang 222005, PR China

ARTICLE INFO

Article history:
Received 4 June 2008
Received in revised form 1 September 2008
Accepted 9 September 2008
Available online 19 September 2008

PACS:
61.10.Nz
68.37.Ps
68.55.-a
73.61.Ga
74.25.Gz

Keywords:
ZnO thin films
TiO_2 buffer layer
Electron beam evaporation
Sol–gel method
Crystalline quality
Photoluminescence

ABSTRACT

In this work, TiO_2 buffer layers were first deposited on Si substrates by electron beam evaporation, and then ZnO thin films were deposited on TiO_2 buffer layers by electron beam evaporation and a sol–gel method, respectively. The structural features and surface morphologies of these films were analyzed by X-ray diffraction (XRD) and a scanning probe microscope (SPM), respectively. The photoluminescence (PL) spectra were measured by a fluorophotometer. The analyses of the structures and surface morphologies showed that all the ZnO thin films were preferentially oriented along the *c*-axis perpendicular to the substrate surface; TiO_2 buffer layers increased the intensity of (0 0 2) diffraction peaks, made the grains denser and the surfaces of the films smoother. The photoluminescence spectra showed that TiO_2 buffer layers enhanced ultraviolet emissions and reduced visible emissions of the ZnO thin films to a large degree. All the results suggested that the use of TiO_2 buffer layers effectively improved the quality of ZnO thin films.

1. Introduction

ZnO is an important compound semiconductor with high chemical and thermal stability. It has a wide band gap of 3.37 eV and a large exciton binding energy of 60 meV at room temperature [1]. Many research results show that ZnO has high excitonic emission efficiency, so it is an ideal material for the fabrication of short-wavelength optoelectronic devices. So far, ZnO is still studied mainly in the form of thin films. ZnO thin films have potential applications in ultraviolet light-emitting diodes [2], ultraviolet lasers [3], ultraviolet photoconductive detectors [4], thin film transistors [5] and so on. A lot of research results show that the optical and electrical properties of ZnO thin films have a direct connection with their crystalline quality. Therefore, if we want to obtain ZnO-based optoelectronic devices with good performance, we must prepare good quality ZnO thin films first. However, the quality of ZnO thin films is closely connected with the substrate materials. Up to now, ZnO thin films have deposited on many substrate materials such as sapphire, SiO_2, Si, quartz, glass, GaAs, MgO, etc. Compared with other substrate materials, Si possesses some advantages like abundant source and mature preparation technique of single crystal Si. In particular, the Si material is the cornerstone of the current semiconductor microelectronics industry. If high quality ZnO thin films are prepared on Si substrates, it will be beneficial for effective integration of optoelectronic devices with Si IC technology. However, when ZnO thin films are being deposited on Si substrates or annealed at high temperature, Si atoms on the substrate surface are easy to "capture" oxygen atoms from ZnO thin films [6], which makes oxygen vacancies in the films increase greatly and consequently deteriorates the quality of the ZnO thin films. Therefore, many researchers have used buffer layers between ZnO thin films and Si substrates to improve the quality of ZnO thin films. Some groups used the homogeneous buffer layer [7] and still others used the heterogeneous buffer layers such as CaF_2 [8], MgO [9], SiC [10], Ti [11], etc.

In previous work, our group prepared the ZnO/TiO_2 thin film on a quartz substrate by electron beam evaporation [12], and found the TiO_2 layer improved the crystalline quality of the ZnO thin film.

* Corresponding author. Tel.: +86 25 84315592; fax: +86 25 84314916.
E-mail addresses: congyu3256@tom.com, congyu3256@sina.com (L. Xu).

0169-4332/$ – see front matter © 2008 Elsevier B.V. All rights reserved.
doi:10.1016/j.apsusc.2008.09.026

In this work, we prepared ZnO/TiO_2 thin films on Si substrates. That we chose TiO_2 as a buffer layer material is based on the following considerations. (1) Both TiO_2 and ZnO are wide-band-gap materials. They have some similar properties such as high chemical and thermal stability, high refractive indices. TiO_2 and ZnO thin films have high transmittance in the visible region, whereas they have intense absorption in the ultraviolet band. What's more, nanostructures of TiO_2 and ZnO such as nanoparticles, nanofilms and so on have good photocatalytic efficiency. (2) TiO_2 is abundant and low cost, so it is suitable for TiO_2 to be used in actual production. (3) By consulting literatures, we had learned high quality TiO_2 thin film had been deposited on a ZnO buffer layer [13]. Therefore, we suppose that a TiO_2 buffer layer will also probably improve the quality of a ZnO thin film grown on a Si substrate. In previous work, some groups have investigated the photocatalytic property of ZnO/TiO_2 thin films [14,15]. In this study, TiO_2 buffer layers were first deposited on Si substrates by electron beam evaporation, and then ZnO thin films were deposited on TiO_2 buffer layers by electron beam evaporation and a sol–gel method, respectively. We studied the structural and photoluminescence properties of ZnO thin films with and without a TiO_2 buffer layer, and at the same time made a comparison between the ZnO thin films deposited on TiO_2 buffer layers by electron beam evaporation and the sol–gel method, respectively.

2. Experiments

2.1. Deposition of TiO_2 buffer layers and ZnO thin films by electron beam evaporation

TiO_2 buffer layers and ZnO thin films were prepared by electron beam evaporation (PMC90S, Protech Korea Ltd.). High purity (99.999%) ZnO and TiO_2 particles were used as source materials. The substrate material is Si (1 0 0). Si substrates were first rinsed in acetone and ethanol, respectively, with ultrasonic vibration for 5 min. Then the substrates were put into diluted HF solution for 3 min to remove SiO_2 layers and finally rinsed in deionized water. The substrate temperatures were 200 °C and 250 °C, respectively, for deposition of TiO_2 buffer layers and ZnO thin films. The deposition chamber was pumped down to 2.66×10^{-3} Pa before deposition. When a TiO_2 layer was deposited, Ar (18 sccm) and O_2 (25 sccm) were introduced into the chamber (working pressure: 1.1×10^{-2} Pa). The electron gun voltage and working current were 7.11 kV and 246 mA, respectively. Afterwards, ZnO thin films were deposited on a Si substrate and a TiO_2 buffer layer, respectively. The corresponding deposition parameters were as follows. Ar (18 sccm) and O_2 (50 sccm) were used and the working pressure was 2.67×10^{-2} Pa. The electron gun voltage was 7.11 kV and the working current was 78 mA. The thicknesses of the TiO_2 buffer layer and the ZnO thin film were 200 and 300 nm, respectively. The ZnO thin film deposited on the Si substrate was labeled sample A and that one deposited on the TiO_2 buffer layer was labeled sample B. Both sample A and B were annealed at 600 °C in air for 1 h.

2.2. Deposition of a ZnO thin film on the TiO_2 buffer layer by the sol–gel method

Zinc acetate, ethanol and monoethanolamine were used to prepare ZnO sol. The concentration of zinc acetate was 0.35 mol/L. The ZnO sol was aged for 24 h at room temperature and then a ZnO thin film was deposited on the TiO_2 buffer layer by a spin-coating method. The spin-coating time was 30 s. In the former 10 s, the rotary speed was 1000 rpm; in the latter 20 s, the rotary speed was 2000 rpm. After each coating, the film was put into a furnace at 300 °C to be dried and given a pre-heat treatment for 5 min. The procedure from coating to drying was repeated several times to make the thickness of the ZnO thin film reach ~300 nm. At last, the film was annealed at 600 °C in air for 1 h. This film was labeled sample C.

2.3. Characterization of microstructure and photoluminescence of the ZnO and ZnO/TiO_2 thin films

The crystal phase and crystalline orientation of the films were analyzed by an X-ray diffractometer (Bruker D8 Advance, Cu Kα λ = 0.15406 nm). The surface morphologies were observed by a scanning probe microscope (CSPM4000) in AFM mode. The photoluminescence spectra were measured by a fluorophotometer. The excitation source was a Xe lamp; the excitation wavelength was 325 nm. All the measurements were carried out at room temperature in air.

3. Results and discussion

3.1. The structures and surface morphologies of the ZnO and ZnO/TiO_2 thin films

Fig. 1 shows the XRD patterns of ZnO and ZnO/TiO_2 thin films. The entire ZnO thin films show only one diffraction peak which corresponds to the diffraction of (0 0 2) plane of ZnO with a hexagonal wurtzite structure. This means all the ZnO thin films deposited on the Si substrate or TiO_2 buffer layers are preferentially oriented along the c-axis perpendicular to the substrate surface. For the sample A, B and C, their (0 0 2) peaks lie at 34.65°,

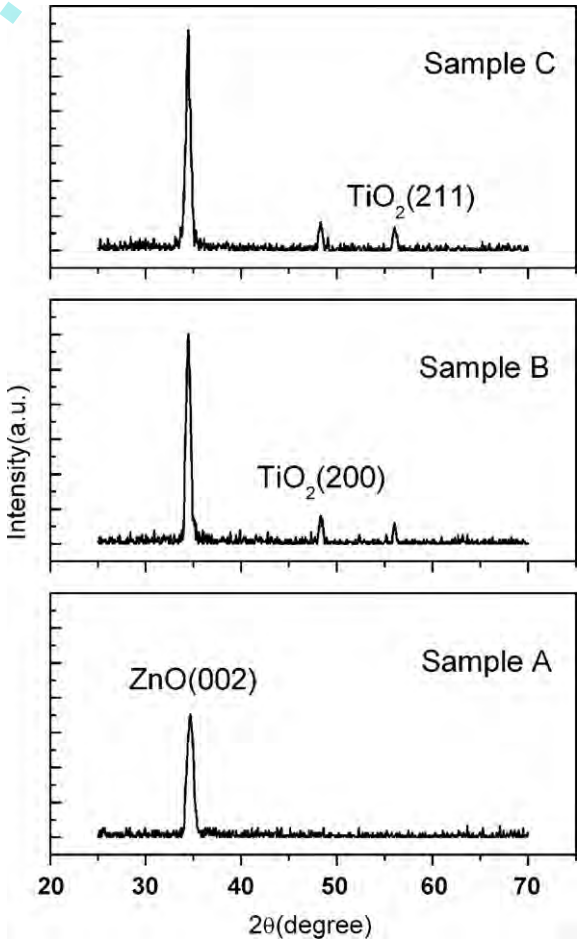

Fig. 1. XRD patterns of ZnO and ZnO/TiO_2 thin films.

34.46° and 34.45°, respectively. The position of the (0 0 2) peak is connected with the strain in a ZnO thin film. The strain often results from deformation of crystal lattices as a result of the existence of many point defects. As for strain-free ZnO powder, its (0 0 2) peak lies at 34.43° [16]. From the above data, it is clear that the (0 0 2) peak positions of ZnO/TiO_2 thin films are closer to the (0 0 2) peak position of ZnO powder than that of ZnO thin film grown on the Si substrate. This indicates TiO_2 buffer layers make the strains in the ZnO thin films decrease. It is probably because TiO_2 buffer layers prevent Si atoms on the substrate surface from "capturing" oxygen atoms from the ZnO thin films and as a result point defects like oxygen vacancies in the films greatly reduced. What is more, the strain change is also related to the lattice and thermal mismatch between ZnO and substrate. The lattice and thermal mismatch between ZnO and Si (1 0 0) are 40% and 45%, respectively; the counterpart between ZnO and anatase-structured TiO_2 are 14% and 9.2%, respectively. Therefore, the decrease of lattice and thermal mismatch is another reason for the reduced strain of ZnO/TiO_2 films. According to the order of sample A, B, and C, the intensity of their (0 0 2) peaks gradually increases in sequence, but the full width at half maximum (FWHM) of the peaks gradually decreases. It means the crystalline quality of ZnO thin films is improved after TiO_2 buffer layers are used. The average crystallite sizes of the ZnO thin films can be calculated with Scherrer formula using parameters derived from XRD patterns. Scherrer formula is as follows:

$$D = \frac{0.9\lambda}{\beta \cos\theta}$$

where D is the crystallite size, λ is the X-ray wavelength, β is the FWHM and θ is the diffraction angle. For the sample A, B and C, their crystalline sizes are 12.1, 17.6 and 18.5 nm, respectively. As regards the sample B and C, there are not only the (0 0 2) peaks of ZnO thin films but also two peaks of TiO_2 layers in the patterns. One of them corresponds to the (2 0 0) diffraction peak (48.30°) of anatase phase, another corresponds to the (2 1 1) peak (56.05°) of rutile phase. But the main components of TiO_2 layer are anatase-structured crystals.

Fig. 2 displays the surface morphologies of the samples. From Fig. 2, it can be seen that all the samples have granular and uniform grains. However, the grain sizes observed by the atomic force microscope are different from those calculated with Scherrer formula. This is because AFM analysis yields information based on surface features while XRD probes the film "bulk" properties [17].

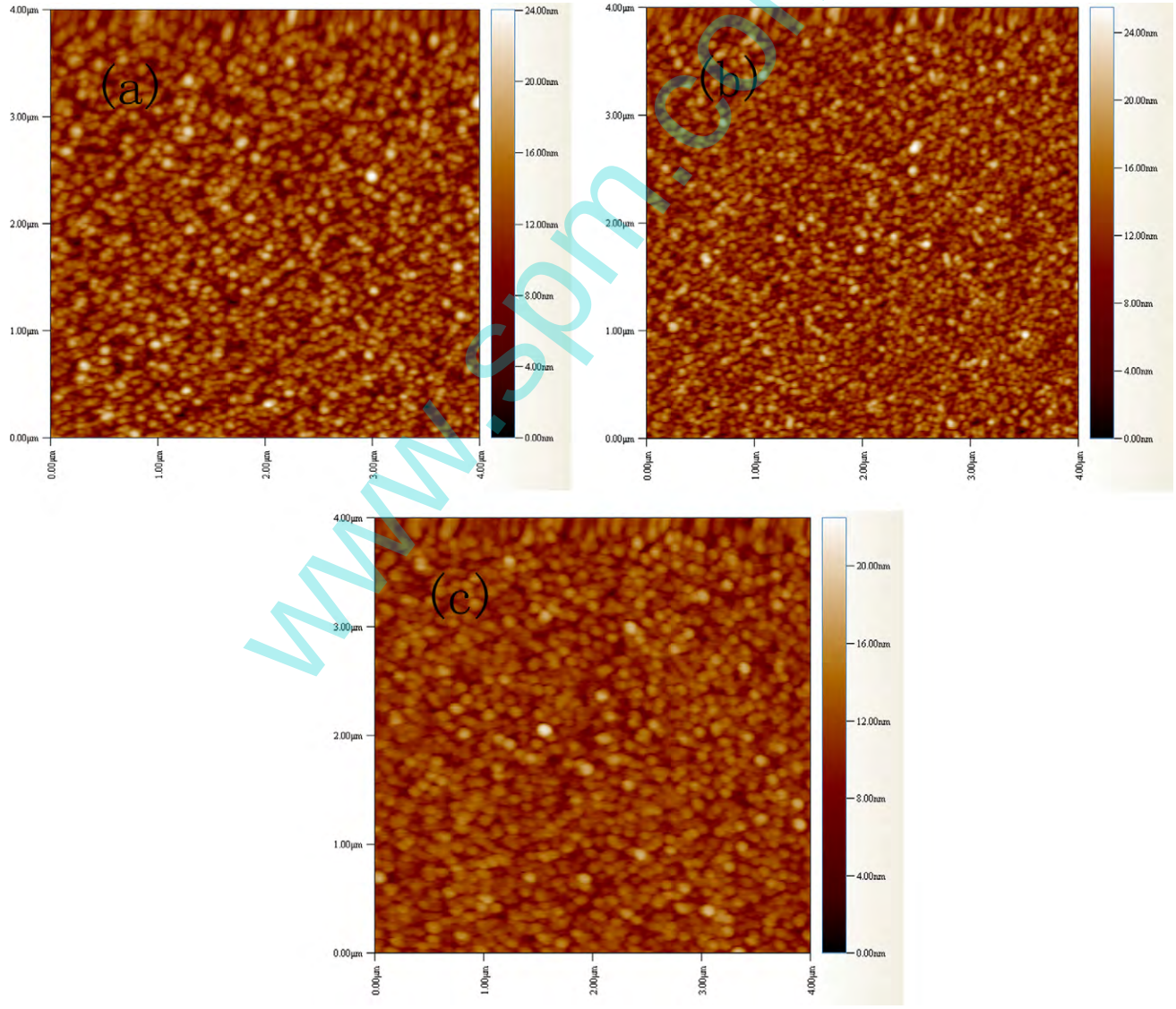

Fig. 2. Surface morphologies of ZnO ((a): Sample A) and ZnO/TiO_2 thin films ((b): Sample B and (c): Sample C).

Compared with the ZnO thin film grown on the Si substrate, those grown on TiO_2 buffer layers have smoother surfaces and denser grains. The average surface roughnesses are 2.03, 1.84 and 1.62 nm for sample A, B and C, respectively. Although both sample B and C are the ZnO thin films deposited on TiO_2 buffer layers, it can be seen from Fig. 2 that their in-plane grains are different. The grains of the ZnO thin film deposited by the sol–gel method on the TiO_2 buffer layer is a little bigger than that of the ZnO thin film deposited by electron beam evaporation on the TiO_2 buffer layer. It is probably connected with the two different deposition methods. For the electron beam evaporation method, the ZnO thin film is continuously deposited on a substrate. When the growth temperature is relatively low, the growth of grains takes place mainly in the annealing treatment. However, as for the sol–gel method, the ZnO thin film must be dried and given a pre-heat treatment after each coating. During the pre-heat treatment, some grains are formed and start to grow. When the total coatings are finished and the film is post-annealed at a relatively high temperature, the grains will grow bigger than ever.

3.2. The photoluminescence property of the ZnO and ZnO/TiO_2 thin films

Fig. 3 shows the PL spectra of the samples. From Fig. 3, it is clear that the three samples have different photoluminescence behavior. For the ZnO thin film deposited on the Si substrate, it has not only an ultraviolet emission peak centered at 381 nm but also a green–yellow emission band centered at 542 nm. For the ZnO thin film deposited by electron beam evaporation on the TiO_2 buffer layer, it has a stronger ultraviolet emission, but its green emission decreases greatly and emission center shifted to 528 nm. As for the ZnO thin film deposited by the sol–gel method on the TiO_2 buffer layer, it has the strongest ultraviolet emission among the samples, and has almost no visible emission.

With respect to the ultraviolet emission centered at 381 nm of ZnO thin films, it is generally considered it results from recombination of free exciton [18,19]. Therefore, the ultraviolet emission is closely connected with the density of free exciton in ZnO thin films. As we know, the density of free exciton is directly associated with the crystalline quality of the films—only ZnO thin films with good quality and low defects density could have high density of free exciton. Therefore, from the results of the photoluminescence, it can be drawn a conclusion that TiO_2 buffer layers improved the crystalline quality to some extent. Furthermore, the enhanced ultraviolet emission from ZnO thin films grown on TiO_2 buffer layers is also probably connected with fluorescence resonance energy

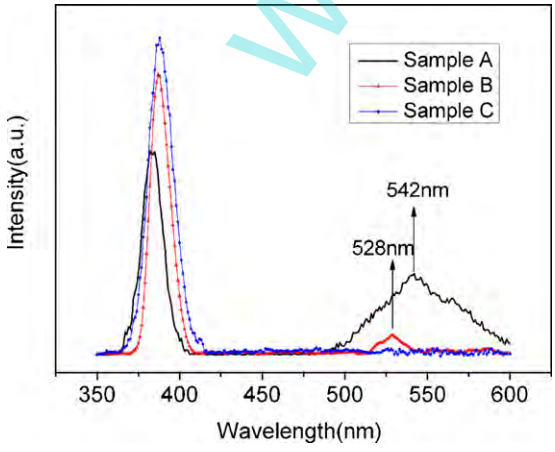

Fig. 3. PL spectra of ZnO and ZnO/TiO_2 thin films.

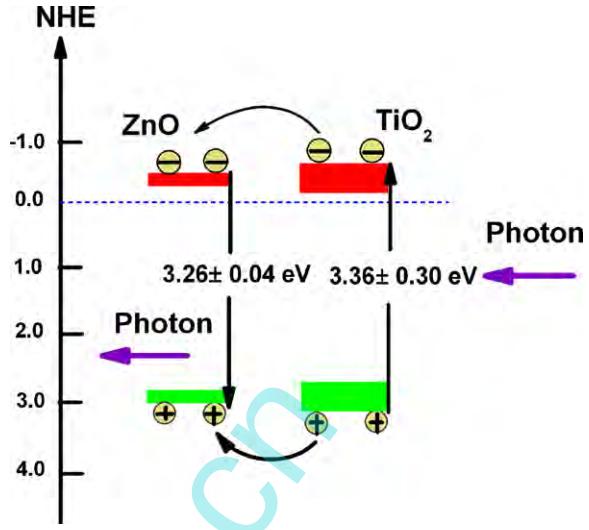

Fig. 4. Energy band alignment of ZnO/TiO_2 composite.

transfer (FRET) between ZnO and TiO_2 [20]. Fig. 4 shows the energy band alignment of ZnO/TiO_2 composite [20]. After the excitation of electron–hole pairs in TiO_2 layer, through the resonance effect, the energy is easily transferred to ZnO thin films [20]. As a result, the band gap emission of ZnO is enhanced. The more detailed explanation about FRET is in literature [20]. As for the green emission of ZnO thin films, it is a relatively common phenomenon, but its emission mechanism is controversial as yet. Some researchers think the green emission results from oxygen vacancies in ZnO thin films [21–23], some ascribe the green emission to oxygen interstitials [24], and still others think the green emission corresponds to the local level composed by oxide antisite defect rather than oxygen vacancy or oxygen interstitial [16,25]. But none of the opinions has been verified directly yet. We tend toward the green emission mainly resulting from oxygen vacancies. For ZnO thin films deposited by electron beam evaporation, the existence of oxygen vacancies probably results from two cases. Firstly, when ZnO thin films are being deposited on Si substrates or annealed at relatively high temperature, Si atoms on the substrate surfaces are easy to "capture" oxygen atoms from ZnO thin films [6], leading to many oxygen vacancies in the films. Secondly, during the growth of ZnO thin films, Zn and O are non-stoichiometric (This case often happens in ZnO thin films deposited by physical deposition method such as pulsed laser deposition, magnetron sputtering, electron beam evaporation and so on). For sample A, it has a relatively strong green emission; its oxygen vacancies are connected with both the above-mentioned two cases. With respect to sample B, because the TiO_2 buffer layer has prevented Si atoms from capturing oxygen atoms from the ZnO thin film, its oxygen vacancies are mainly produced during the film growth. As regards the ZnO thin film deposited by the sol–gel method on the TiO_2 buffer layer, it has almost no green emission. This means ZnO thin films deposited by liquid phase techniques such as sol–gel method have a good stoichiometry. It should be noted that the green emission center of sample B shifted compared with that of sample A. The phenomena of the shift of green emission center also occurred in Al doped ZnO thin films [26,27] and the ZnO thin film on a SiC buffer layer [10]. Especially, for the ZnO thin film deposited on the SiC buffer layer by Zhang et al., its green emission center also shifted toward short-wavelength direction compared with that of the ZnO thin film deposited on the Si substrate. Zhang et al. [10] think the shift of deep level emission from ZnO films on Si and SiC buffer layer may be attributed to the different defect centers associated to the stress,

strain and dislocation in samples. So far, we can't still give a better explanation about this phenomenon. In order to find out the reason, more detailed work is being carried out.

4. Conclusions

TiO_2 buffer layers were first deposited on Si substrates by electron beam evaporation, and then ZnO thin films were deposited on TiO_2 buffer layers by electron beam evaporation and the sol–gel method, respectively. The analyses of structures show that all the ZnO thin films are preferentially oriented along the c-axis perpendicular to the substrate surface. TiO_2 buffer layers increased the intensity of (0 0 2) peaks, improved the crystalline quality of ZnO thin films. All the ZnO thin films have granular and uniform grains. Those films deposited on TiO_2 buffer layers have smoother surface and denser grains. The photoluminescence spectra indicate that the ZnO thin film deposited on the Si substrate has an ultraviolet emission and a relatively strong green emission while those films on TiO_2 buffer layers have stronger ultraviolet emissions and weaker green emissions. It is mainly because TiO_2 buffer layers prevent Si atoms from "capturing" oxygen atoms from ZnO thin films. As a result, the point defects like oxygen vacancies in the films decreased greatly; thus the quality of ZnO thin films were improved. Furthermore, the enhanced ultraviolet emission from ZnO/TiO_2 thin films is also probably associated with FRET between ZnO and TiO_2. In view of the various applications of ZnO/TiO_2 thin films, in the following work, we will study the effect of TiO_2 buffer layer thickness and annealing temperature on the structural and optical properties of ZnO thin films.

References

[1] Z.W. Li, W. Gao, J. Roger, Reeves, Surf. Coat. Technol. 198 (2005) 319.
[2] W. Liu, S.L. Gu, J.D. Ye, S.M. Zhu, S.M. Liu, X. Zhou, R. Zhang, Y. Shi, Y.D. Zheng, Y. Hang, C.L. Zhang, Appl. Phys. Lett. 88 (2006) 092101.
[3] A. Mitra, R.K. Thareja, V. Ganesan, A. Gupta, P.K. Sahoo, V.N. Kulkarni, Appl. Surf. Sci. 174 (2001) 232.
[4] Z.-Q. Xu, H. Deng, J. Xie, Y. Li, X.-T. Zu, Appl. Surf. Sci. 253 (2006) 476.
[5] K. Lee, J.H. Kim, S. Im, C.S. Kim, H.K. Baik, Appl. Phys. Lett. 89 (2006) 133507.
[6] X.M. Fan, J.S. Lian, Z.X. Guo, H.J. Lu, Appl. Surf. Sci. 239 (2005) 176.
[7] D.J. Park, J.Y Lee, T.E. Park, Y.Y. Kim, H.K. Cho, Thin Solid Films 515 (2007) 6721.
[8] K. Koike, T. Komuro, K. Ogata, S. Sasa, M. Inoue, M. Yano, Physica E 21 (2004) 679.
[9] M. Fujita, M. Sasajima, Y. Deesirapipat, Y. Horikoshi, J. Crystal Growth 278 (2005) 293.
[10] Y. Zhang, H. Zheng, J. Su, B. Lin, Z. Fu, J. Lumin. 124 (2007) 252.
[11] F. Li, D. Li, J. Dai, H. Su, L. Wang, Y. Pu, W. Fang, F. Jiang, Superlatt. Microstruct. 40 (2006) 56.
[12] L. Shi, H. Shen, L. Jiang, X. Li, Mater. Lett. 61 (2007) 4735.
[13] M.H. Cho, G.H. Lee, Thin Solid Films 516 (2008) 5877.
[14] Z. Zhang, Y. Yuan, Y. Fang, L. Liang, H. Ding, L. Jin, Talanta 73 (2007) 523.
[15] D.W. Kim, S. Lee, H.S. Jung, J.Y. Kim, H. Shin, K.S. Hong, Int. J. Hydrogen Energy 32 (2007) 3137.
[16] P. Sagar, P.K. Shishodia, R.M. Mehra, H. Okada, A. Wakahara, A. Yoshida, J. Lumin. 126 (2007) 800.
[17] V. Khranovskyy, R. Minikayev, S. Trushkin, G. Lashkarev, V. Lazorenko, U. Grossner, W. Paszkowicz, A. Suchocki, B.G. Svensson, R. Yakimova, J. Crystal Growth 308 (2007) 93.
[18] S. Cho, J. Ma, Y. Kim, Y. Sun, K.L. Wong George, B. Ketterson John, Appl. Phys. Lett. 75 (1999) 2761.
[19] Y. Zhang, B. Lin, Z. Fu, C. Liu, W. Han, Opt. Mater. 28 (2006) 1192.
[20] H.Y. Lin, Y.Y. Chou, C.L. Cheng, Y.F. Chen, Opt. Express 15 (2007) 13832.
[21] K. Vanheusden, C.H. Seager, W.L. Warren, D.R. Tallant, J.A. Voigt, Appl. Phys. Lett. 68 (1996) 403.
[22] J.S. Kang, H.S. Kang, S.S. Pang, E.S. Shim, S.Y. Lee, Thin Solid Films 443 (2003) 5.
[23] F.K. Shan, G.X. Liu, W.J. Lee, B.C. Shin, J.Appl. Phys. 101 (2007) 053106.
[24] Y. Liu, J. Lian, Appl. Surf. Sci. 253 (2007) 3727.
[25] B. Lin, Z. Fu, Y. Jia, Appl. Phys. Lett. 79 (2001) 943.
[26] M. Wang, K.E. Lee, S.H. Hahn, E.J. Kim, S. Kim, J.S. Chung, E.W. Shin, C. Park, Mater. Lett. 61 (2007) 1118.
[27] G. Srinivasan, R.T. Rajendra Kumar, J. Kumar, Opt. Mater. 30 (2007) 314.